GEOSCIENCES REVIEW

GeoRev is a free access journal of the Department of Geology, Bayero University, Kano, Ngeria

Assessment of Water Quality Index in Densely Populated Areas of Jos Metropolis Central, Nigeria

Yakubu, J. A., Kucheti, J. E. & Dibal, H. U.
Department of Geology, University of Jos

ARTICLE INFORMATION ABSTRACT www.georev.org

Article history:
Received 30 October 2025
Revised 17 December 2025
Accepted 19 January 2026
Available online 24 February 2026

Keywords:
Water Quality Index
Contamination
Metropolis
Jos
Domestic use

Water quality index refers to the quality of a given water sample represented by its index number that indicates the general water quality for various intended uses. The study aims to assess the water quality index in densely populated low-income areas of Jos metropolis. Thirty-three (33) water samples were collected from hand-dug wells (26 from high-population-density areas and 7 from low-population-density areas) using 100 mL sanitized water bottles. A BWB XP flame photometer was utilized to analyze the anions, a HACH DR1900 portable spectrophotometer was used to analyze major ions, while HCO_3^- was determined by the titrimetric method. In the biological analysis, total coliform count, total plate count, and their isolates were determined by membrane filtration. The weighted arithmetic method was used for the computation of the water quality index. The chemical parameters in the area showed that $Na^+ > Mg^{2+} > K^+ > Ca^{2+}$ for the cations and $HCO_3^- > Cl^- > SO_4^{2-} > NO_3^-$ for the anions. Results obtained from the water quality index showed that 15.2% of the water samples were excellent, 24.2% were of good quality, 18.2% were of poor water quality, 15.2% were of very poor quality, while 27.2% were unsuitable for drinking. There is no variation for these water quality indices irrespective of the population density. The water quality index showed that 72% of the water is potable for drinking, whereas 28% is not potable. The presence of pathogenic and indicator organisms in most of the water samples may render it unfit for human consumption without proper treatment.

Peer review under the responsibility of the Department of Geology, Bayero University, Kano. ©
Corresponding author. E-mail address: yajubujanet247@gmail.com (J. A. Yakubu). DOI: 0000-0002-3482-998x.

INTRODUCTION

Globally, groundwater is the most abundant source of liquid freshwater on Earth, underpinning water supplies for drinking, sanitation, and agriculture. It is estimated to provide half the volume of water withdrawn for domestic use by our global population, including the vast majority of drinking water for the rural dwellers, making it especially critical for communities across Sub-Saharan Africa (UN-Water, 2022).

The public water supply in urban centers like Jos Metropolis is under intense pressure due to low investment and non-maintenance of existing infrastructure, lack of morale-boosting initiatives for personnel, and a negative public attitude towards social services. Although the public is obliged to pay for water delivery services, economically disadvantaged and low-income households pose a significant barrier to meeting this commitment. As a result, low-income families, particularly those residing in densely populated areas, are cut off from the public water supply, resulting in the exploitation of underground water for drinking, domestic, and other uses. The irregularity of public water supply is also responsible for the use of groundwater in most industries and

households across the metropolis. Groundwater remains the bedrock of secure drinking water supplies across Sub-Saharan Africa, forming the primary source for both rural and urban populations. Its reliability and natural protection from contamination make it a cornerstone strategy for achieving Sustainable Development Goal 6 (clean water and sanitation), with numerous urban centers relying on it either partially or entirely to meet their daily water demands (World Bank, 2022).

In the study area (Tudun Wada and Anguwan Rogo), there is an increase in anthropogenic activities due to an increase in population. Pit latrines and local drainage systems, among other contamination sources, are a key source of groundwater contamination in low-income countries. Contamination was found to be most severe in shallow aquifers, with high concentrations of E. coli and nitrate detected within 10-50 meters of latrines (Graham & Polizzotto, 2021).

This study aims to assess the suitability of groundwater for human consumption and domestic purposes by determining its Water Quality Index (WQI).

Description of the study area

The study area is situated in Jos and defined by Latitudes 9˚51'46" - 9˚57'56" North and Longitudes 8˚50'44" - 8˚54'33" East. The area of coverage extends from Angwan Rukuba towards the Air Force Base and from FGC Jos to State Low-cost, as shown in Figure 1. A significant repercussion of the Jos Plateau is that it controls its climate, which differs from the surrounding plains. The climate of Jos Plateau is typical of the tropical zone type. A more recent climatic analysis shows that the Jos Plateau experiences a mean annual rainfall ranging from approximately 1200mm to over 1500mm, with significant local variation influenced by topography (Fasona et al., 2021; PNCC, 2022).

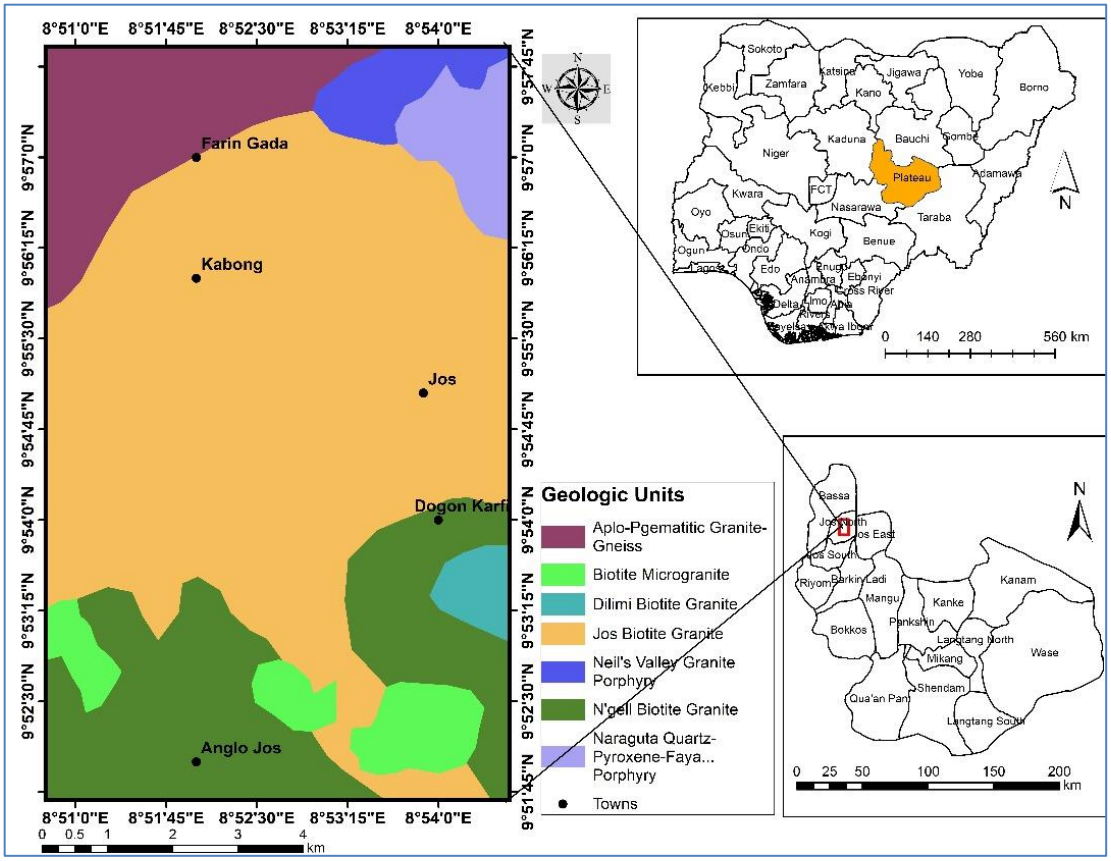

Figure 1: Map of the study area subset from the map of Plateau State and Jos North LGA

Geology of the Study Area

The geology of the Jos Plateau comprises the Precambrian Basement migmatite gneiss-quartzite complex underlying approximately half of the Plateau, and some areas have been intruded by Precambrian to late Paleozoic Pan-African granite (Older Granite), diorite, charnockite, etc. Intrusive into these Basement Complex rocks are the Jurassic anorogenic alkali Younger Granites. The Younger Granite province of the Jos Plateau is associated with extensive volcanic

rocks, including basalts and rhyolites, which intrude and overlie both the Younger Granites and the Precambrian Basement Complex. Modern geochronology distinguishes between the "Older Volcanics" (or "Jos Plateau Basalts") of the Cenozoic and the geologically recent, predominantly Quaternary "Newer Basalts," with the latter forming the most prominent and well-preserved volcanic features (Dada et al., 2021; Afolayan et al., 2022). The geology of the study area, situated within the Jos-Bukuru Complex, is predominantly underlain by biotite granite of the Jurassic Younger Granite province. This composition has been confirmed and characterized in detail by recent geological mapping and petrological studies (Dada & Ganev, 2020; Garba et al., 2021), as presented in Figure 2.

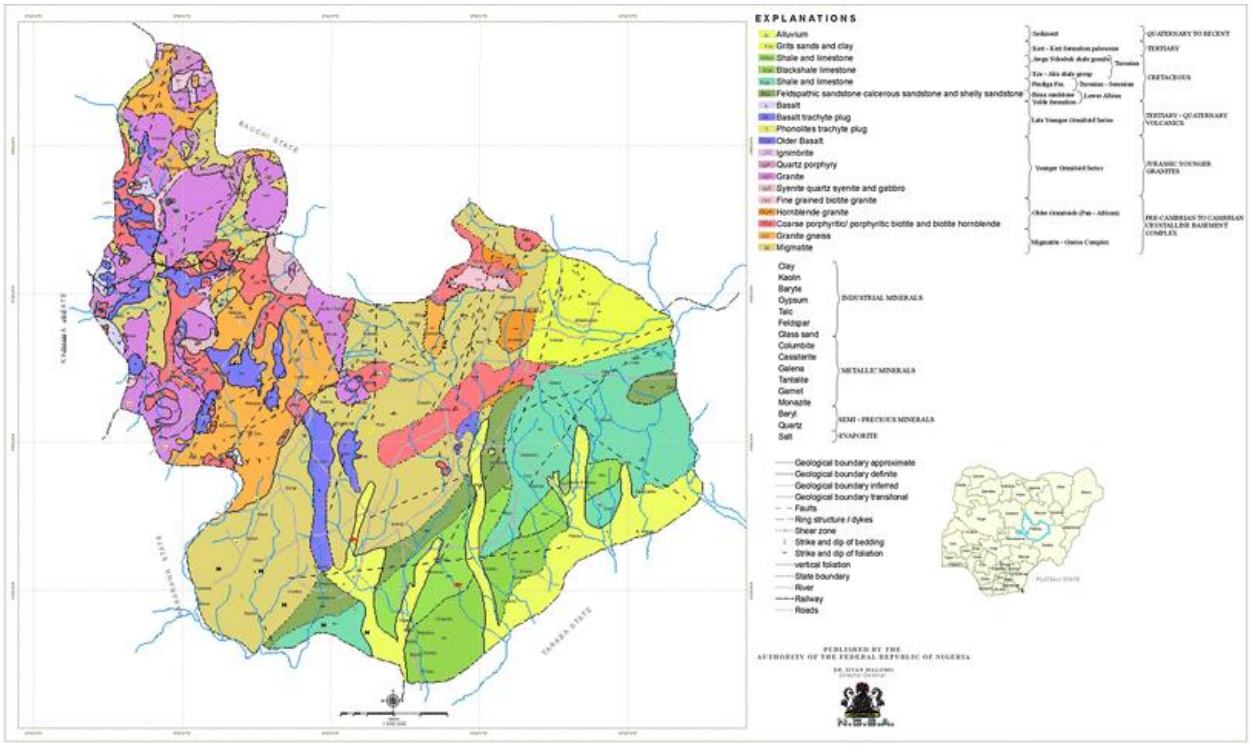

Figure 2: Geological Map of Plateau State (Geological Survey of Nigeria, GSN, 2006)

MATERIALS AND METHODS

The random field sampling approach, primarily focused on groundwater observation and data collection, as adopted by Freeze & Cherry (1979), was used in this research. Groundwater samples from hand-dug wells were collected from thirty-three (33) locations in Jos metropolis during the peak of the dry season in April 2023. The 100cl water bottles were rinsed with distilled water and 1% of HNO_3 and allowed to dry before use. Three (3) samples were collected at each location: the first for anion analysis, the second for cation analysis, and the third for the biological analysis. Two (2) drops of nitric acid (HNO_3) were added to the samples meant for cation analyses to avoid bacterial growth and to keep the ions in solution. Groundwater samples were collected from evenly distributed hand-dug wells following standard protocols to minimize turbidity and ensure representative sampling. The procedure involved retrieving water using a clean, dedicated plastic container (APHA, 2017; British Geological Survey, 2017). A hand-held measuring tape was used to determine the depth of the water level of the wells. Field parameters such as pH, temperature, and conductivity were determined using the HACH pH/temperature meter by dipping the meter into the sampling pail, and the values were taken once the reading on the meter stabilized.

Sample Preparation and Laboratory Analyses

Water samples were taken to the University of Jos Science Laboratory Technology (SLT) for analysis of cations with particular focus on Ca^{2+}, Mg^{2+}, Na^{+}, and K^{+}. Flame photometry (BWB XP flame photometer) was used to ascertain the concentration of the cations in the sample. The water samples were analyzed for anions such as HCO_3^{-}, SO_4^{2-}, Cl^{-}, and NO_3^{-}. The reason for selecting these cations and anions was that they are potential geogenic and anthropogenic contamination indicators. The HACH DR1900 portable

spectrophotometer was used for the anion analysis. HCO_3^- was determined by the titrimetric method. Samples were taken to the University of Jos Microbiology laboratory for bacteriological analyses. Total coliform count was determined by membrane filtration.

Determination of Water Quality Index (WQI) in the Study Area

The weighted arithmetic water quality index (WQI_A), which was first proposed and adopted by Horton (1965) and developed by Brown *et al.* (1972), was used to calculate the Water quality index (WQI) as shown in equations 1, 2, and 3:

$$WQI_A = \frac{\sum Q_i W_i}{\sum W_i} \text{---------- (1)}$$

The quality rating scale (Qi) for every parameter is calculated using:

$$Q_i = 100\left[\frac{V_i - V_o}{S_i - V_o}\right] \text{---------- (2)}$$

Keys:

V_i = Estimated Concentration of the i^{th} variable of interest in the analysed water.
V_o = The ideal value of the i^{th} variable in pure water.
V_o = 0 (except for pH = 7.0)
S_i = Recommended Standard value of the i^{th} variable.
The unit weight (W_i) for each water quality variable is calculated by using:

$$W_I = \frac{K}{S_i}, \quad K = \frac{1}{\sum\left(\frac{1}{S_i}\right)} \text{---------- (3)}$$

K = proportionality constant. It can be calculated using the simultaneous equation stated above.

RESULTS

Concentration and Distribution of Major Elements and physico-chemical properties of water in the Study Area

The physicochemical parameters of water samples acquired from hand-dug wells in the study area are presented in Table 1. The temperature of the water samples in the study area ranged from 22.5°C to 35.7°C with a mean value of 26.6°C, while the pH ranged from 6.38 to 9.78 with a mean value of 7.9. Fifteen (15) samples out of the 33 water samples, representing 46% of the water samples, ranged from 7 to 7.5.

EC was found to range from 60µS/cm to 3398µS/cm with a mean value of 901.1µS/cm, in 30.3% of the samples, the EC was found to be above 1000µS/cm in areas such as Down Base, Angwan Rimi, Angwan Rogo, New Market, Ali Kazaure, Busa Buji, Tudun Wada, Apata, Congo and Duala Barracks, while the TDS was found to range from 30 to 1699 with a mean value of 444.1, at locations such as Down Base, Angwan Rimi, Angwan Rogo, New Market, Ali Kazaure, Busa Buji, Tudun Wada, Apata, Congo and Duala Barracks, the values were found to be higher than 500 which agrees with the high concentration of EC and this represents 30.3% of the water samples analyzed from the different locations.

The concentration of Calcium (Ca^{2+}) ranged from 0.95mg/L to 318.1mg/L with a mean value of 25.6mg/L. Statistically, 93.9% was found to be below 50mg/L, and an anomalous value of 318.1mg/L was found at Kufang, as shown in Figure 3, while that of Magnesium (Mg^{2+}) ranged from 9.6mg/L to 105.6mg/L with a mean value of 37.2mg/L.

In the samples collected, wells in areas such as Angwan Jarawa, Duala Barracks, Apata, Old Airport, and Ali Kazaure had concentrations above 50mg/l. This represents 15.2% of the total samples collected. The concentration is presented as a distribution map in Figure 4.

Sodium (Na^+) concentration ranged from 2.93mg/L to 347.03mg/L with a mean value of 106.1mg/L. From the data obtained, areas such as Kufang, Sabon-layi II, Angwan Rimi, Nasarawa, Rikkos, Apata, Congo, and Duala Barracks (24.2% of the sampled locations) were observed to have concentrations higher than 200mg/l, as shown in Figure 5.

Furthermore, potassium (K^+) concentration in the water samples ranged from 0.83mg/L to 217.87mg/L with a mean value of 28.2mg/L. Duala Barracks, Congo, Katako Market, Apata, Tudun Wada III, Tudun Wada II, Kufang, Abbatoir, Tudun Osi, Nasarawa, Angwan Rukuba, New Market, Angwan Rimi, Sabon Layi II, ECWA staff, and Miango State Low-cost have potassium concentration above 12mg/L. Figure 6 shows the concentration of this element in the water samples collected from these areas. The concentration of these cations in the water samples in descending order is $Na^+ > Mg^{2+} > K^+ > Ca^{2+}$.

The concentration of Bicarbonate (HCO_3^-) ranges from 24.2mg/L to 951.6mg/L with a mean value of 172.1mg/L. The samples obtained from Duala Barracks and Apata were observed to be considerably high (above 400mg/l), as shown in Figure 7.

Table 1: Physicochemical parameters in waters of the study area

Sample	T	pH	EC	TDS	Ca^{2+}	Mg^{2+}	Na^{+}	K^{+}	HCO_3	SO_4^{2-}	Cl^{-}	NO_3
Unit	^0C	-	mS/m	Mg/L	Mg/L	Mg/L	Mg/L	Mg/L	Mg/L	Mg/L	Mg/L	Mg/L
WHO/SON (2017)	25	7	1000	500	75	50	200	12	400	200	250	50
State low-cost	27.2	7.21	68	34	20.70	48.00	132.67	23.57	366.00	90.10	215.99	21.77
K Beside NYSC	26.4	7.35	73	36	318.10	28.80	224.67	51.70	195.20	109.87	214.00	31.47
Down base	27.8	9.02	2100	1050	1.40	9.60	6.93	3.90	122.00	1.07	21.90	-
ECWA Staff	29.2	9.78	254	127	24.70	48.00	94.69	47.27	336.00	69.13	159.95	6.37
Sabon Layi 1	30.2	7.8	83	41	2.50	38.40	6.60	3.40	73.20	1.33	23.85	3.53
Sabon Layi 2	28.8	8.7	266	113	32.40	28.80	284.87	29.60	122.00	29.93	233.90	12.90
Anguwan Rimi	29.0	9.7	2270	1130	37.60	48.00	240.23	217.87	195.20	22.00	267.92	19.40
Anguwan Rogo	30.4	9.55	2172	1040	0.95	38.40	2.93	2.23	73.20	1.33	33.34	2.07
New Market	29.2	9.61	2459	1103	2.85	28.80	184.87	39.80	219.60	56.40	141.55	24.27
Ali Kazaure	30.2	9.12	2078	1039	1.20	105.60	5.00	0.83	73.20	1.07	19.20	3.267
Busa Buji	26.7	12.2	1850	920	1.20	19.20	5.20	1.57	48.80	0.97	19.66	0.700
Anguw Rukuba	25.0	7.5	650	313	32.25	38.40	80.13	24.63	146.40	45.13	25.74	20.50
Nasarawa	26.5	8.05	860	440	35.00	19.20	217.90	25.00	244.00	15.00	91.45	6.033
Tudun Osi	35.1	8.02	730	381	15.50	28.80	69.97	20.43	390.40	22.00	109.99	1.210
Gangare	26.1	7.4	144	72	2.05	28.80	7.90	8.47	73.20	4.93	217.93	1.200
Rik NDLEA Jun	27.1	7.92	852	417	31.60	19.20	222.93	12.73	122.00	3.13	19.56	12.27
Abbatoir	25.5	6.38	486	238	7.90	9.60	70.00	21.60	146.40	0.90	203.66	37.63
Old Airport	35.7	6.65	60	30	1.20	57.60	6.03	0.83	48.80	12.77	79.98	3.70
Opp NASCO	24.6	7.17	174	87	6.00	9.60	26.30	3.03	24.40	0.07	21.55	9.65
Kufang	27.2	7.10	610	305	30.15	28.80	82.73	22.70	73.20	42.93	45.89	14.40
Tudun Wada 1	25.0	6.6	518	247	9.30	38.40	57.93	9.10	24.40	2.93	105.67	24.21
Tudun Wada 2	26.1	7.31	1458	729	88.00	48.00	199.90	45.47	122.00	57.10	69.29	44.20
Tudun Wada 3	24.5	6.45	732	368	24.50	28.80	83.00	21.87	48.40	0.13	227.91	34.90
GSS Kabong	24.2	7.24	230	115	2.70	38.40	23.77	4.50	73.20	1.00	23.45	7.767
Rukuba Road	22.5	7.13	220	110	3.10	19.20	20.83	4.80	48.80	1.17	204.00	25.000
Apata	23.6	7.35	1494	747	25.35	67.20	347.03	25.50	414.80	41.17	25.99	2.653
Busa Buji 2	24.6	7.45	184	93	2.55	28.80	12.97	3.93	48.80	0.00	91.88	11.177
Katako market	23.9	7.03	570	285	18.90	38.40	70.90	14.13	24.40	3.30	217.83	20.200
Congo	24.7	7.3	1826	913	25.00	19.20	323.07	23.20	390.40	4.00	263.12	2.567
Duala Barracks	23.3	7.55	3398	1699	33.20	76.80	327.93	206.83	951.60	57.10	409.88	-
Anguw Jarawa	22.7	7.53	404	202	3.05	57.60	25.83	3.80	170.80	5.71	39.33	-
Kunyi Katse	23.3	7.62	158	79	1.55	38.40	7.27	3.03	170.80	2.73	13.45	2.167
Fa Gada Market	22.7	7.14	306	153	2.70	48.00	28.30	4.53	97.60	1.20	281.34	4.967
Mean	26.6	7.9	901.1	444.1	25.6	37.2	106.1	28.2	172.1	21.4	125.5	13.7

Key: High-density areas are left in black, Low-density areas (control areas) are colored blue

Sodium (Na^{+}) concentration ranged from 2.93mg/L to 347.03mg/L with a mean value of 106.1mg/L. From the data obtained, areas such as Kufang, Sabon-layi II, Angwan Rimi, Nasarawa, Rikkos, Apata, Congo, and Duala Barracks (24.2% of the sampled locations) were observed to have concentrations higher than 200mg/l, as shown in Figure 5. Furthermore, potassium (K^{+}) concentration in the water samples ranged from 0.83mg/L to 217.87mg/L with a mean value of 28.2mg/L. Duala Barracks, Congo, Katako Market, Apata, Tudun Wada III, Tudun Wada II, Kufang, Abbatoir, Tudun Osi, Nasarawa, Angwan Rukuba, New Market, Angw Rimi, Sabon Layi II, ECWA staff, and Miango Low-cost have K concentration > 12mg/L.

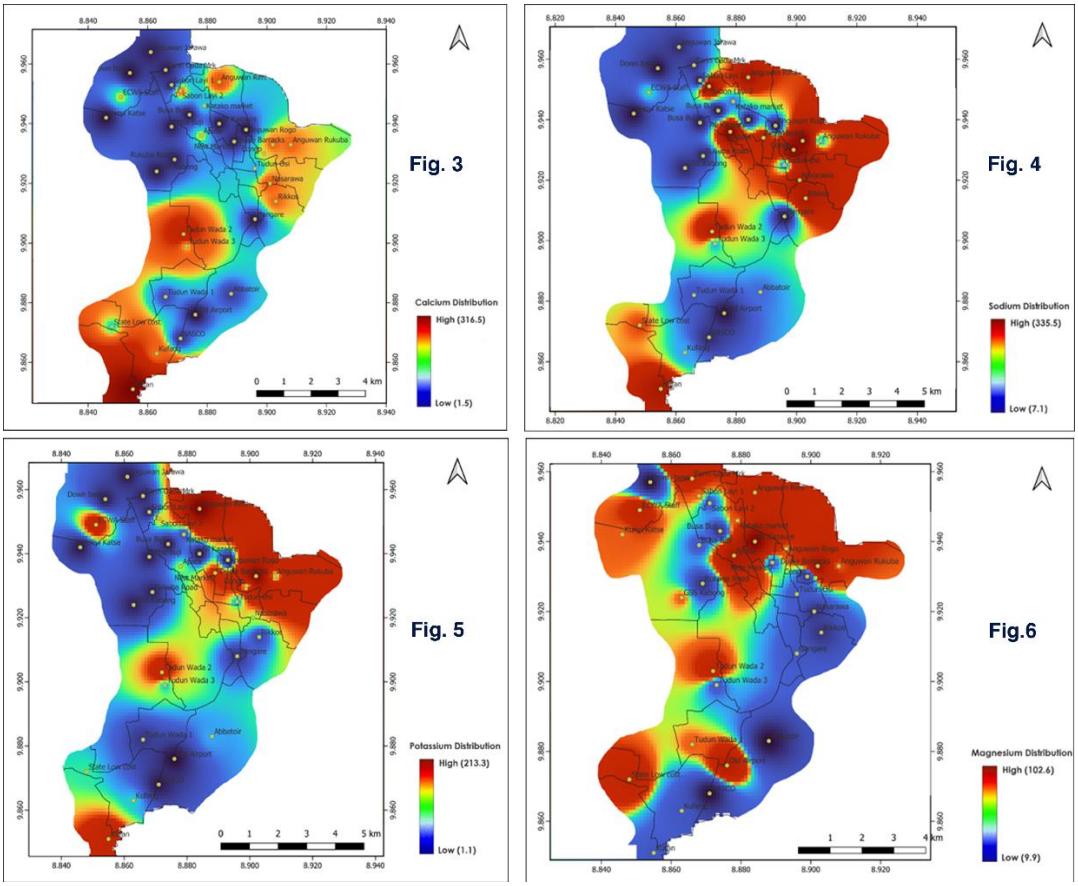

Figures 3, 4, 5 & 6: Spatial Distribution map of Calcium, Sodium, Potassium & Magnesium in the study area.

Figure 6 shows the concentration of this element in the water samples collected from these areas. The concentration of these cations in the water samples in descending order is $Na^{+} > Mg^{2+} > K^{+} > Ca^{2+}$.

The concentration of Bicarbonate (HCO_3^-) ranges from 24.2mg/L to 951.6mg/L with a mean value of 172.1mg/L. The samples obtained from Duala Barracks and Apata were observed to be considerably high (above 400mg/l), as shown in Figure 7.

The concentration of Sulphate (SO_4^{2-}) ranges from 0.07mg/L to 109.9mg/L with a mean value of 21.4mg/L as presented in Figure 8. Chloride (Cl^-) concentration ranges from 13.5mg/L to 409.9mg/L with a mean value of 125.5mg/L.

Within the study area, sampled wells with high concentrations of chloride above 250mg/l were found in locations such as Miango State, low-cost, Angwan Rimi, Congo, Duala Barracks, and Farin Gada Market (Figure 9).

Furthermore, nitrate (NO_3^-) concentration ranged from 0.7mg/L to 44.2mg/L with a mean value of 13.7mg/L as shown in Figure 10.

The concentration of the anionic species in groundwater in the study area was in this order: $HCO_3^- > Cl^- > SO_4^{2-} > NO_3^-$.

Biological Content of Waters

Table 2 presents the biological composition of the collected water. These include Total Plate Count (TPC), Total Coliform Count (TCC), and microorganisms found in these samples.

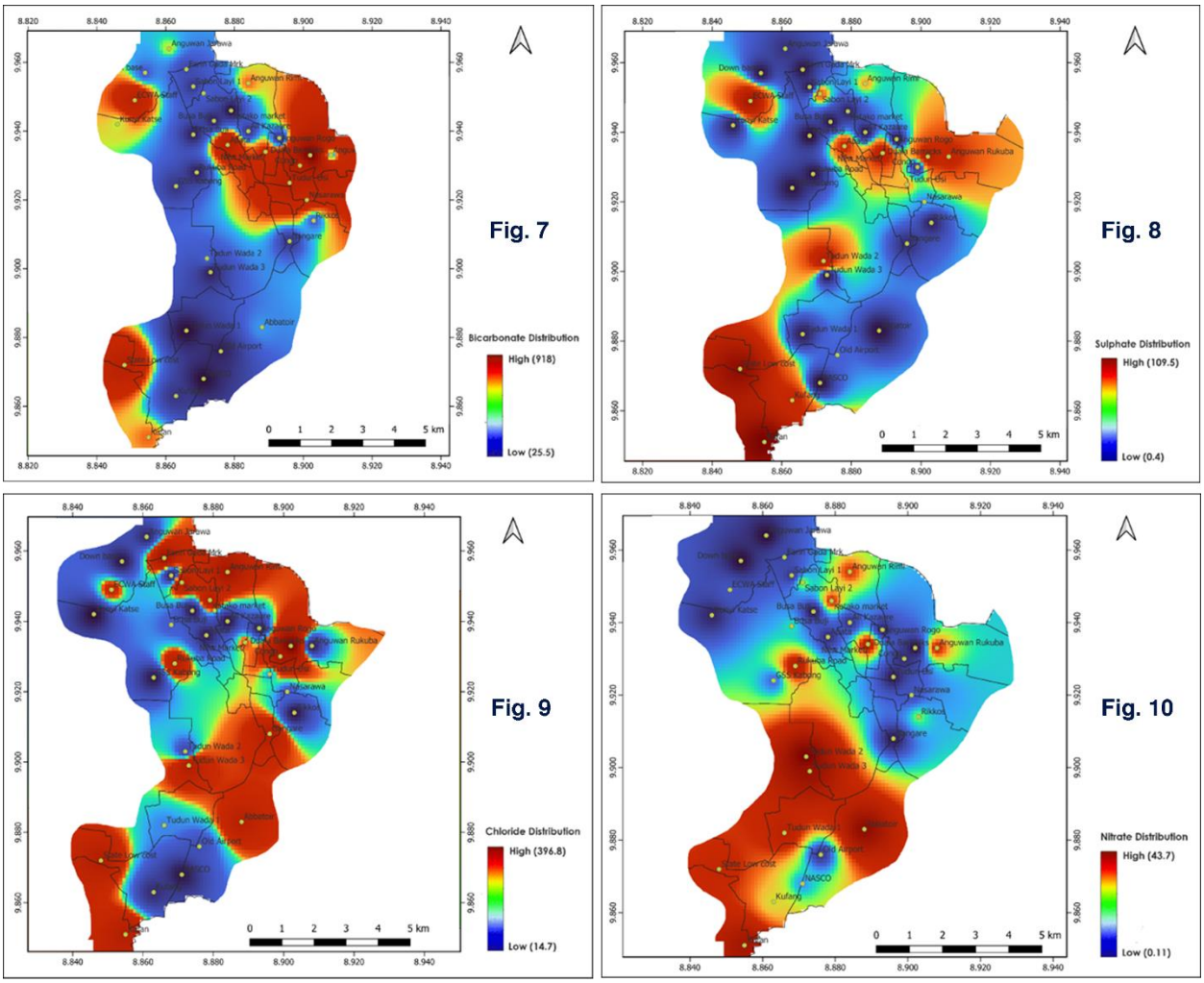

Figures 7, 8, 9 & 10: Spatial Distribution map of Bicarbonate, Sulphate, Chloride & Nitrate

From the bacteriological analysis presented in Table 2, TPC in excess of 100mls of the samples were found in Down-Base, Tudun Wada, and Angwan Rukuba, which represents 9.1% of the samples. About 60.6% of the samples were found to be high (above 10 per 100ml). These samples were collected at Miango State, low-cost, Kufang Beside NYSC, ECWA staff, Sabon-Layi, Anguwan Rimi, Anguwan Rogo, New Market, Busa Buji, Abattoir, Opposite NASCO, Kufang, Tudun Wada, GSS Kabong, Rukuba Road, Apata, Busa Buji, and Farin Gada Market. Furthermore, the TCC of samples from Tudun Wada 1 was uncountable and flooded, which represents 3.1% of the total samples. Other samples that were of high value (above 10 per 100mls) were ECWA staff, Tudun Osi, Opposite NASCO, Kufang, GSS Kabong, Apata, and Congo; these represent 21.2% of the samples. The micro-organisms isolated from the water samples included Staphylococcus aureus, which was found in 9.1% of the samples at locations such as Angwan Rogo, Ali Kazaure, and Tudun Wada 2. Another micro-organism found in 48.5% of the samples was Escherichia coli (E. Coli), found at locations such as Miango State, low-cost, ECWA staff, Sabon Layi 2, Anguwan Rimi, Anguwan Rogo, Nasarawa, Rikkos NDLEA junction, Opp. NASCO, Tudun Wada 2, Tudun Wada 3, GSS Kabong, Apata, Busa Buji 2, Congo, Anguwan Jarawa, and Farin Gada Market. This was the most prevalent microorganism in the water samples. Protus species were found in 18.2% of the analyzed samples at locations such as Nasarawa, Old Airport, Kufang, Tudun Wada 1, Duala Barracks,

and Anguwan Jarawa. Additionally, Salmonella species were found to be prevalent in 24.2% of the samples in areas such as New Market, Ali Kazaure, Tudun Osi, Gangare, Abattoir, Old Airport, Kufang, and Katako market. Streptococcus Faecalis was found in 21.2% of the samples at locations such as State-low cost, Kufang Beside NYSC, Sabon Layi 1, Busa Buji, Rikkos NDLEA junction, and Rukuba Road. Another micro-organism found in the samples was Pseudomonas Aeruginosa, which was found in 15.2% of the samples at locations such as Kufang beside NYSC, Sabon Layi 1, Sabon Layi 2, Busa Buji, and Katako market. Shigella Spp was found in 15.1% of the samples in areas such as Down base, Sabon layi 1, New market, Opposite NASCO, and Rukuba road. Also, Bacillus Spp was found in 15.1% of the samples at locations such as Down base, Sabon layi 1, Gangare, GSS Kabong, and Kunyi-Katse.

Piper Trilinear Diagram

The interpretation of hydro-chemical facies will not be complete without employing the Piper trilinear diagram (Piper, 1944). Hydro-chemical facies and the evolutionary trends of groundwater are commonly interpreted using graphical methods, where samples with similar characteristics cluster into distinct groups, visually illustrating their similarities and differences (Appelo & Postma, 2022). Hydro-chemical facies are distinct zones within an aquifer with characteristic chemical compositions, resulting from the complex interplay of mineral dissolution kinetics, flow patterns, water-rock interaction, and residence time (Fetter et al., 2018; Appelo & Postma, 2022). The diamond-shaped section of the diagram explains how groundwater is classified. Ca^{2+} and Mg^{2+} are regarded as alkaline earths, while Na^{+} and K^{+} are regarded as alkalis among the primary cations. Cl^{-} and SO_4^{2-} ions are classified as strong acids, while HCO_3^{-} and CO_3^{2-} anions are classified as weak acids. Figure 10, which is the Piper Trilinear diagram of the analysed water samples, shows that 13 samples out of 33, representing 39.4% (W001, W002, W004, W009, W012, W014, W015, W019, W021, W025, W027, W029, and W033), fall into Zone III, which is the Mixed water type. Furthermore, 8 samples out of 33 (W003, W005, W008, W010, W011, W024, W031, and W032) fall into zone II, showing that 24.2% of the groundwater samples are Magnesium Bicarbonate water type.

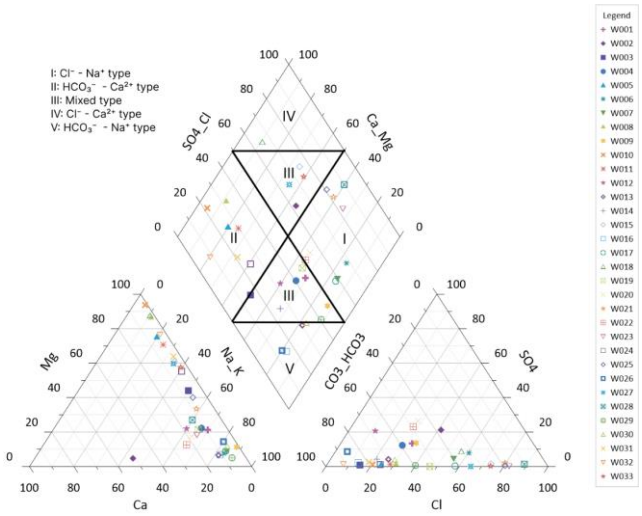

Cations Anions

Figure 10: Piper trilinear diagram showing groundwater hydrochemical facies in the thirty-three (33) water samples collected.

In 7 samples out of 33 (W006, W007, W017, W020, W022, W023, and W028), which represent 21.2% of the samples, are sub-classified in zone I as Sodium Chloride water type. In comparison, 4 of the 33 samples, representing 12.1% (W013, W016, W026, and W030), fall into zone V as Sodium Bicarbonate type. In addition, just 1 out of 33 samples, i.e., 3% (W018), falls into zone IV as Calcium Chloride water type.

Gibbs Plot of the Samples

Gibbs' diagram (Gibbs, 1970) highlights three different sources, such as the rainfall dominant zone, the evaporation dominant zone, and the weathering dominant zone, from which groundwater originates. Gibb's diagram is explained based on two ratios: cation and anion, relative to TDS. The Gibbs diagram of the groundwater in the study area is shown in Figure 11.

Where;

Ratio I (cation) = $(Na^{+} + K^{+})/(Na^{+} + K^{+} + Ca^{2+})$
Ratio II (anion) = $Cl^{-}/(Cl^{-} + HCO_3^{-})$

Table 2: Biological Analysis Results

Sample ID	Site Name	TPC/CFU	TCC/CFU	Micro Org.	Remarks
W001	Miango State low-cost	11	9	B, E	Unsatisfactory
W002	Kufang Beside NYSC	31	1	E, F	Fair
W003	Down base	Num	2	G, H	Unsatisfactory
W004	ECWA Staff	16	12	B	Unsatisfactory
W005	Sabon Layi 1	27	3	E, F, G, H	Unsatisfactory
W006	Sabon Layi 2	35	2	B, F	Unsatisfactory
W007	Anguwan Rimi	16	4	B	Unsatisfactory
W008	Anguwan Rogo	22	1	A, B	Fair
W009	New Market	35	6	D, G	Unsatisfactory
W010	Ali Kazaure	2	3	A, D	Fair
W011	Busa Buji	10	2	E, F	Fair
W012	Anguwan Rukuba	Flood	-	Yeast Cells	Fair
W013	Nasarawa	3	2	B, C	Unsatisfactory
W014	Tudun Osi	8	19	D	Unsatisfactory
W015	Gangare	4	8	H, D	Unsatisfactory
W016	Rikkos NDLEA Junction	6	2	B, E	Fair
W017	Abbatoir	14	3	D	Unsatisfactory
W018	Old Airport	3	9	C, D	Unsatisfactory
W019	Opposite NASCO	42	30	B, G	Unsatisfactory
W020	Kufang	30	17	C, D	Unsatisfactory
W021	Tudun Wada 1	Swams	Flood	C	Unsatisfactory
W022	Tudun Wada 2	13	2	A, B	Fair
W023	Tudun Wada 3	20	4	B	Unsatisfactory
W024	GSS Kabong	15	12	E, H, B	Unsatisfactory
W025	Rukuba Road	21	7	E, G	Unsatisfactory
W026	Apata	31	22	B	Unsatisfactory
W027	Busa Buji 2	16	9	B	Unsatisfactory
W028	Katako market	17	1	D, F	Fair
W029	Congo	7	20	B	Unsatisfactory
W030	Duala Barracks	4	6	C	Unsatisfactory
W031	Anguwan Jarawa	9	2	B, C	Unsatisfactory
W032	Kunyi Katse	6	2	H	Fair
W033	Farin Gada Market	11	9	B	Unsatisfactory

Keys: A = Staphylococcus Aureus, B = Escherichia Coli, C = Protus Species, D = Salmonella Species, E = Streptococcus Faecalis, F = Pseudomonas Aeruginosa, G = Shigella Spp, H = Bacillus Spp

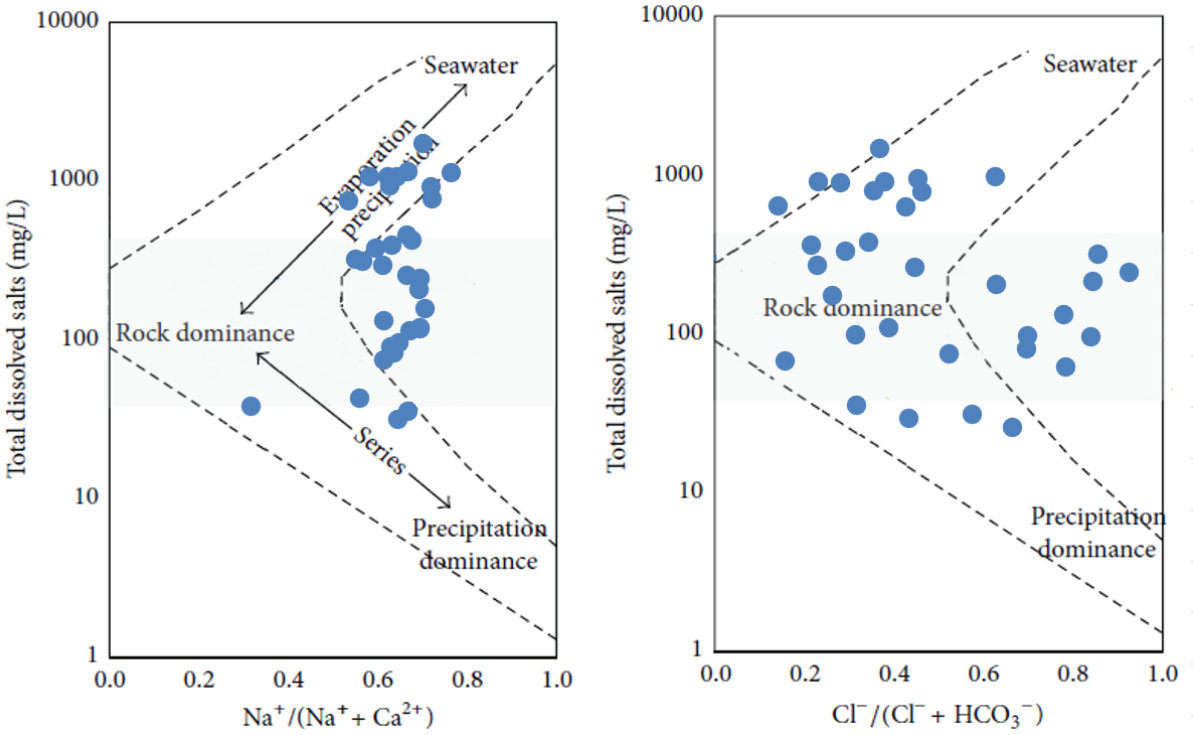

Figure 11: Gibbs plot showing groundwater interaction in the study area (Gibbs, 1970).

A critical factor in deciphering groundwater quality and origin is the water-rock interaction between aquifer minerals and subsurface water, a fundamental process controlling solute acquisition and evolution along flow paths (Appelo & Postma, 2022).

From the Gibbs plot in Figure 11, on the TDS vs Gibbs ratio I, 36.4% of the water samples (12 locations) were found to be of rock dominance, 57.6% of the water samples (19 locations) plotted on the portion of evaporation, and 6.1% of the samples (2 locations) plotted in the precipitation zone. On the other hand, on the TDS versus Gibbs ratio II, 57.6% of the water samples (19 locations) plotted in the region of rock dominance, 30.3% of samples (10 locations) plotted on the side of evaporation, while 12.1% of the samples (4 locations) were found to be plotted in the region of precipitation.

Correlation coefficient analysis of chemical parameters

Pearson correlation coefficient analysis is a fundamental statistical approach for establishing the strength and direction of linear relationships between numerical hydrochemical parameters.

By quantifying the correlations between various physicochemical parameters and the ionic content of groundwater, this method provides critical insights into the governing geochemical processes, such as rock-water interactions, ion exchange, and anthropogenic influences. The analysis effectively distinguishes the degree of association between independent and dependent variables, helping to identify the key factors controlling groundwater chemistry (Adimalla et al., 2020; Selvakumar et al., 2017; Zhang et al., 2021). The correlation coefficient (r) refers to the degree of interdependence of two or more parameters and is typically used to assess the relationship between variables.

When the values are r ≅ +1 or -1, respectively, the relationship between the two variables is considered and related to a positive or negative linear correlation. There will be no correlation between the two variables when r≅ 0. Variables with positive correlation are those with a common source, while those emanating

from different sources are said to have negative correlation.

Table 3: Correlation coefficient matrix between major ions in the study area.

	pH	EC	TDS	Ca^{2+}	Mg^{2+}	Na^{+}	K^{+}	HCO	SO	Cl^{-}	NO
pH	1										
EC	0.499477	1									
TDS	0.49041	**0.998725**	1								
Ca	-0.10477	-0.09148	-0.08821	1							
Mg	0.025491	0.281057	0.290401	-0.04384	1						
Na	-0.017	0.401367	0.403317	0.391641	0.098417	1					
K	0.156971	**0.545061**	**0.554006**	0.22483	0.284889	**0.575154**	1				
HCO	0.017578	0.481166	0.492752	0.117559	0.331969	**0.638191**	**0.628053**	1			
SO_4	0.029868	0.050623	0.042972	0.658795	0.203378	0.498853	0.380864	0.482266	1		
Cl	-0.1908	0.148959	0.152722	0.204581	0.051962	0.440001	**0.584809**	0.479223	0.273991	1	
NO	-0.3388	-0.15116	-0.16304	0.409894	-0.21865	0.158565	0.104551	-0.22814	0.331544	0.232233	1

Variables having r >0.7 or -0.7 will be termed strongly correlated, and values ranging from 0.5 to 0.7 or -0.5 to -0.7 will be considered to have moderate correlation (Adimalla & Qian, 2021; Karunanidhi et al., 2021). From Table 3, it can be observed that there is a positive correlation (+0.998725) between EC and TDS, and also a positive of (+0.545061) between EC and potassium (K^{+}). Furthermore, TDS shows a positive correlation of (0.554006) with K^{+}. Na^{+} shows a positive correlation of 0.575154 and 0.638191 with K^{+} and HCO_3, respectively. Also, K^{+} shows a positive correlation of 0.628053 with HCO_3 and 0.584809 with chloride.

The population figures were projected by the authors using the formula $P_{2023} = P_{2006}(1 + r)^n$, where ($P_{2006}$) is the base population, and an annual growth rate (r) for Plateau State is of 3.2%, as provided by the National Bureau of Statistics, was applied over 17 years (n).

Table 4 and Figure 12 show the relationship between the population density of the various wards in the study area and the water quality found in these wards. These wards have been grouped based on the range of population, which shows lower population in the outskirts, ranging from 1,017 to 2,838, compared to the most densely populated area with a range of 18,510 to 20,216. Wards such as Angwan Rogo/Rimi, with an estimated population of 43,546 people (National Bureau of Statistics, 2020), had water samples with varying quality at the various sampled sites, where Angwan Rimi had a WQI of 349.28, Farin Gada Market had a WQI of 25.92, Sabon Layi 1 had a WQI of 38.47, and Angwan Rogo had a WQI of 87.89.

DISCUSSION

Composition of Groundwater and Contribution of Geology

The physicochemical quality of groundwater in the study area is governed by a combination of geogenic processes and anthropogenic influences (Alpha & Orhan, 2017). The Gibbs plot (Figure 11) shows that the majority of samples fall within the rock dominance field, indicating that chemical weathering of aquifer minerals is the primary process shaping hydrochemistry.

This is further supported by the strong geochemical correlations. The very strong positive correlation between TDS and EC (r = +0.9) is expected, given that EC is a direct indicator of dissolved ions. More significantly, TDS shows strong positive correlations with K^{+} and Na^{+}, suggesting these ions are major contributors to the salinity and dissolved load (Zhang et al., 2021; Karunanidhi et al., 2022). This is consistent with the local geology, which contains K-feldspars and biotite minerals characteristic of the Pan-African granitoids, such as the biotite granites

documented within the Jos Plateau Complex (Turner & Bowden, 2021). The positive correlations between HCO_3^- and both Na^+ and K^+ (r = +0.6) reinforce that silicate weathering (e.g., from plagioclase feldspars) is a key driver of water chemistry, also contributing to the alkalinity.

Table 4: Comparison of Population Density in Relation to Water Quality Index in the study area

S/No	Ward	Sample Site	Population	Water Quality Index
1	Angwan Rogo/Rimi	Angwan Rimi	43,546	433.89
2		Farin Gada Market		44.51
3		Sabon Layi 1		23.70
4		Angwan Rogo		17.59
5	Dashonong	Miango State Low-cost	43,306	83.82
6		Kufang		99.76
7	Naraguta A	Nasarawa	15,307	63.62
8	Naraguta B	Congo	50,375	109.96
9		Angwan Rukuba		59.70
10		Duala Barracks		423.14
11	Ibrahim Katsina	Tudun Osi	8,657	99.48
12	Jenta Apata	Apata	32,618	123.91
13		Busa Buji		76.18
14		Sabon Layi 2		74.25
15		Katako Market		42.43
16	Ali Kazaure	Ali Kazaure	13,507	27.59
17		New Market		104.68
18	Hwolshe	Hwolshe/T wada 1	19,086	297.27
19	Gangare	Gangare	7,317	46.12
20	Lamingo	Rikkos	75,415	40.75
21	Gyel B	Kufang NYSC	105,951	128.24
22	Tudun Wada	Tudun Wada 2	52,268	111.67
23		Tudun Wada 3		65.92
24	Kabong	GSS Kabong	89,350	50.51
25		Rukuba Road		38.21
26		Kunyi Katse		20.33
27		Busa Buji 2		40.89
28	Giring	Old Airport	43,751	37.24
29		NASCO		93.08
30		Abbatoir		59.96
31	Ahwol	Down Base	63,056	20.13
32		Ecwa Staff		133.86
33		Angwan Jawara		24.11

Figure 13 shows a non-linear relationship between population and average WQI per ward, which portrays that an increase in population density doesn't always indicate a high WQI and vice versa.

The Piper diagram corroborates this, showing a prevalence of mixed water types (Ca-Mg-Cl and Ca-Na-HCO_3) and a slight dominance of alkalies (Na^+ + K^+) over alkaline earths, which aligns with the identified importance of Na^+ and K^+. While rock

weathering is dominant, a moderate correlation between Cl^- and K^+ (r = +0.6) suggests an additional, anthropogenic source for Cl-, as its concentration is too high to be sourced solely from biotite leaching.

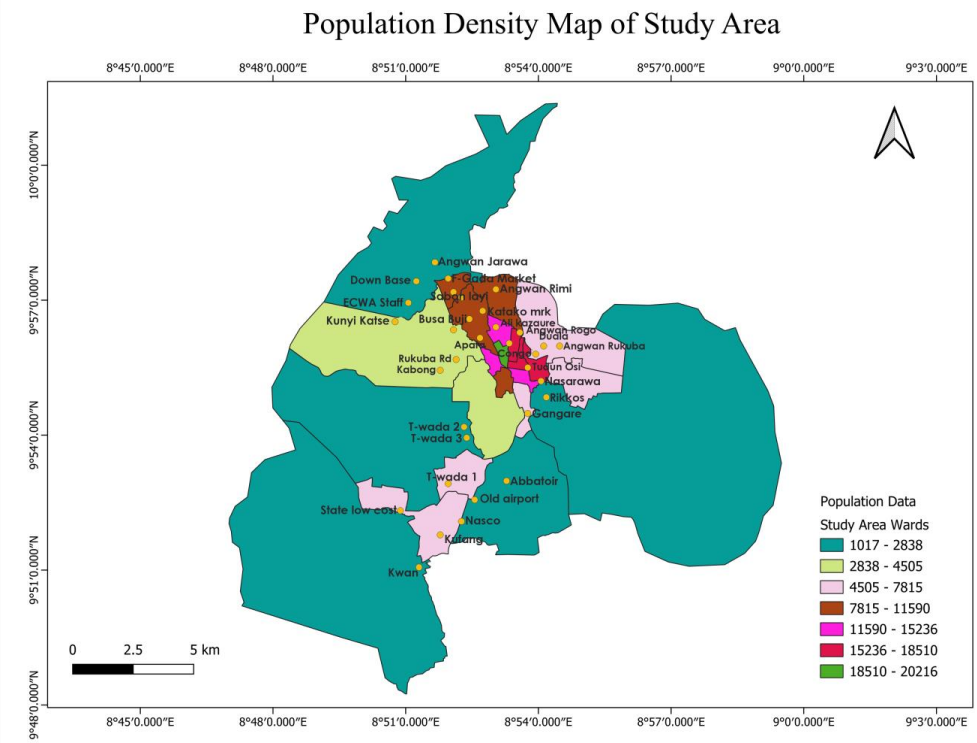

Figure 12: Population Density and Water Quality within the Study Area

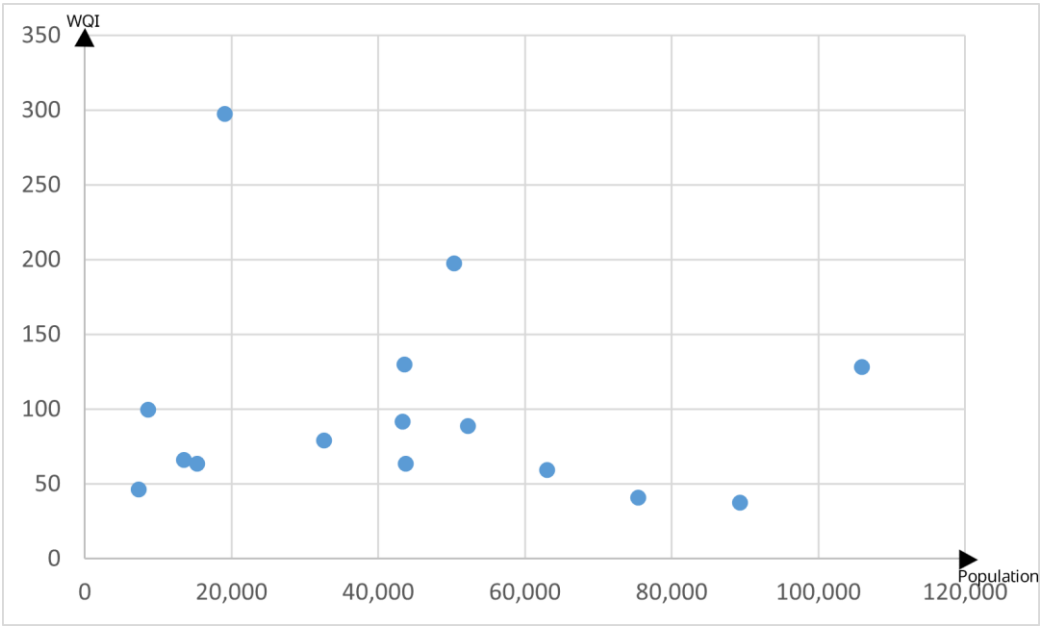

Figure 13: Scatter plot showing the relationship between population and WQI

Composition of Groundwater and Anthropogenic Activities

Anthropogenic activities contribute to groundwater contamination, but its distribution is localized and not solely dependent on population density. This is evident from the scattered occurrence of elevated chemical indicators. High nitrate (>30 mg/L) and sulphate (>50 mg/L) levels were found in a mix of high- and low-density areas, including Tudun Wada, Kufang, and the Abattoir.

Similarly, chloride levels exceeding 200 mg/L were widespread. A clear point source was identified in Miango State, low-cost, where a well was located only 5 meters from a septic tank, indicating likely leaching. Bacteriological contamination further confirms the pervasive but localized nature of pollution. Importantly, 72.73% of samples were found to be bacteriologically unsatisfactory due to the presence of total coliforms, E. coli, Salmonella species, and Streptococcus faecalis. These microbial contaminants were detected across both densely and sparsely populated regions. This even distribution demonstrates that contamination is driven by specific localized activities, such as poor sanitation and proximity to pollution sources like septic tanks, rather than by regional population density alone.

Suitability of Groundwater for Domestic Uses

Domestic water, otherwise known as potable water, is suitable for uses, including but not limited to drinking, laundry, gardening, and other household uses. For this study, we will look at two (2) of these uses: drinking and laundry.

Water for Drinking

Ideally, Potability of drinking water is achieved when the water is free from contaminants and harmful bacteria. The potability of water in the context of its water quality index classification is presented in Table 5 below:

Table 5: Water Quality Classification Based on the Arithmetic WQI Method

WQI	WATER QUALITY STATUS	% OF SAMPLES
0 – 25	Excellent	15.2%
26 – 50	Good Water	24.2%
51 – 75	Poor Water	18.2%
76 – 100	Very Poor Water	15.2%
Above 100	Unsuitable for Drinking	27.3%

Source: Sener et al. (2022); Ustaoglu & Tepe (2023); Tiwari et al., (2021).

The Water Quality Index of the sampled waters, as shown in Table 5, indicates that 15.2% of the water samples are of excellent quality, 24.2% of these waters are classified as of good quality, 18.2% of the water samples are of poor quality, 15.2% are of very poor quality, and 27.2% are unsuitable for drinking.

Figure 14 shows the percentage of water samples based on WQI analyses from the study area that are potable, to be 72.73% compared to 27.27% that did not meet the WQI criteria. The water under review is considered fit for consumption if its WQI < 100, and unfit for drinking if its WQI > 100. However, water quality should not only be ascertained based on the WQI indices alone. (Uddin et al., 2021).

Water for Laundry

Water is universally recognized as the most critical ingredient in the laundering process (McQueen & Terhaag, 2021). The lifespan and appearance of clothing and textiles heavily depend on the quality of water used (Bracken et al.,2021). However, calcium and magnesium are the primary causative agents of hardness in water.

The concentration of Calcium and Magnesium ions, expressed as the equivalent of Calcium Carbonate, is known as the calcium and magnesium hardness. The formula for computing total permanent hardness of

water, expressed as $CaCO_3$, can be calculated as follows:

$$Total\ Hardness\ = 2.5(Ca^{2+}) + 4.1(Mg^{2+})$$

Where the ratios of the atomic weights of Ca^{2+} and Mg^{2+} to the formula weight of $CaCO_3$ are 2.5 and 4.1, respectively.

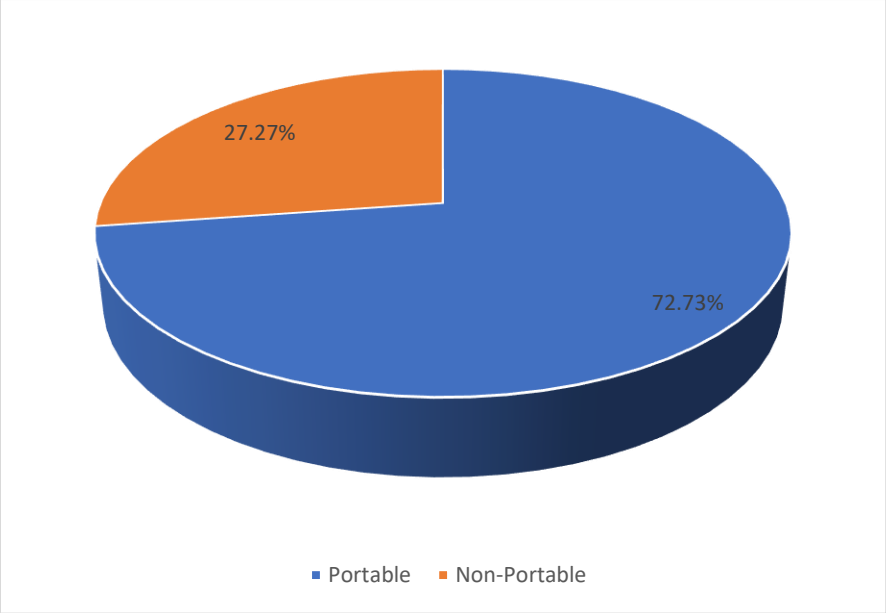

Figure 14: Portability of samples based on the water quality index approach

Table 6: Water Hardness Classification in the study area

Sample ID	Percentage	Hardness Range	Classification	Remark
W003, W017, W019	9.1%	0 – 60	Soft	Excellent
W011, W025	6.1%	61 – 120	Moderate	Good
W005, W008, W009, W013, W014, W015, W016, W023, W024, W027, W029, W032	36.4%	121 – 180	Hard	Needs treatment
W001, W002, W004, W006, W007, W010, W012, W018, W020, W021, W022, W026, W028, W030, W031, W033	48.4%	More than 181	Very Hard	Unsuitable

From Table 6, it is obvious that a higher percentage of the water samples (48.4%) fall under very hard water and can be said to be unsuitable for laundry. This phenomenon can be attributed to the possibility of water being sampled in the height of the dry season, when the concentration of both calcium and magnesium is high. To mitigate the adverse effects of hard water in laundry, several strategies are recommended. These include using liquid detergents with built-in water-softening builders, and most

effectively, employing ion exchange water softeners to remove calcium and magnesium ions at the point of entry. Modern guidelines advise against simply increasing detergent dosage, as this can lead to fabric residue and is environmentally unsustainable (Jiang et al., 2023; American Cleaning Institute, 2021).

CONCLUSION

It is not so much the population density in these areas that were studied that caused water pollution, but the activities of the population that drastically affect the quality of water. This correlates with the conclusion of a study by Digha & Ekanem, 2015, on the effects of population density on water quality in Calabar Municipality, Cross Rivers State. It also aligns with a 2022 study in a Chinese coastal city, which concluded that anthropogenic activities have a more significant impact on river water quality than population density alone (Li et al., 2022).

The results obtained in this research indicate the presence of coliform bacteria, viz, E. coli, Proteus species, Salmonella species, Streptococcus faecalis, Pseudomonas aeruginosa, Shigella spp., and bacillus spp, as well as Staphylococcus aureus in the water samples collected from all the study sites within Jos metropolis. The presence of pathogenic organisms and indicator organisms in most of the water samples may render it unfit for human consumption without proper treatment.

This study sheds light on the need for public health targeted campaigns regarding the dangers caused by drinking untreated water. Well owners need to be educated on affordable water treatment options, such as certified filters or chlorine disinfection systems for bacteria. Enforcement of well construction codes and issuing of permits will help track wells. Geospatial mapping of hotspots of contamination will allow the government to focus intervention initiatives in these areas. There also needs to be funding available for studies focused on tracking groundwater contamination and transport, especially in marginalized rural communities. This will go a long way in improving water quality in every household.

REFERENCES

Adimalla, N., Qian, H., & Tiwari, D. M. (2020). Groundwater chemistry, distribution, and potential health risk appraisal of nitrate-enriched groundwater: A case study from the semi-urban region of South India. *Ecotoxicology and Environmental Safety, 192*, 110305. https://doi.org/10.1016/j.ecoenv.2020.110305

Adimalla, N., & Qian, H. (2021). Groundwater chemistry, distribution and potential health risk appraisal of nitrate enriched groundwater: A case study from the semi-urban region of South India. *Ecotoxicology and Environmental Safety, 192*, 110305. https://doi.org/10.1016/j.chemosphere.2020.128146

Afolayan, O. S., Ganev, V. Y., Asah, T. T., Itiga, O. O., & Dada, S. S. (2022). Petrogenesis and Geodynamic Setting of Quaternary Basalts from the Jos Plateau, Central Nigeria: Constraints from Geochemistry and Isotope Geochemistry. *Geochemistry*, 82(3), 125869. https://doi.org/10.1016/j.chemer.2022.125869

Alpha, B., & Orhan, G. (2017). Effect of Geogenic Factors on Water Quality and Its Relation to Human Health around Mount Ida, Turkey. *Multidisciplinary Digital Publishing Institute*, Basel, Switzerland.

American Cleaning Institute (ACI). (2021). *Laundering in Hard Water: A Guide for Consumers*. Washington, DC. https://www.cleaninginstitute.org/understanding-products/laundering-hard-water-guide-consumers.

APHA, AWWA, WEF. (2017). *Standard Methods for the Examination of Water and Wastewater* (23rd ed.). American Public Health Association. ISBN: 978-0875532875.

Appelo, C. A. J., & Postma, D. (2022). *Geochemistry, Groundwater and Pollution* (3rd ed.). CRC Press. ISBN: 978-0367657501.

Bracken, L., De Malsche, W., De Moor, R. J., & Verwee, E. (2021). The role of water quality on the efficacy of laundry detergents. *Colloids and Surfaces A: Physicochemical and Engineering*

Aspects, 610, 125741. https://doi.org/10.1016/j.colsurfa.2020.125741

British Geological Survey (BGS). (2017). *Groundwater Sampling Methodology.* https://www.bgs.ac.uk/some-folder/specific-document.pdf.

Brown, R. M., McClelland, N. I., Deininger, R. A., & O'Connor, M. F. (1972). *A water quality index for crashing water quality*. National Sanitation Foundation.

Dada, S. S., & Ganev, V. Y. (2020). The Jurassic Younger Granite Province of Northern Nigeria: A review of its geology, geochemistry, and mineralization. In *Geology and Mineral Resources of Nigeria* (pp. 119–142). Springer. https://doi.org/10.1007/978-3-030-40585-2_5

Dada, S. S., Ganev, V. Y., & Babalola, L. O. (2021). *The anorogenic Jurassic and Cenozoic volcanic provinces of Nigeria: A review*. Journal of African Earth Sciences, 179, 104189. https://doi.org/10.1016/j.jafrearsci.2021.104189.

Digha, O. N., & Ekanem, J. D. (2015). Effects of Population Density on Water Quality in Calabar Municipality Cross Rivers State, Nigeria, *Journal of Environment and Earth Science*, *5*(2), 19-20. https://iiste.org/Journals/index.php/JEES/article/view/19447/19918.

Fasona, M., Olajuyigbe, A., Adeonipekun, P., Akande, S., Adegboyega, S., Odunuga, S., Omojola, A., & Soneye, A. (2021). Rainfall variability and its impacts on vegetation dynamics in the Jos Plateau, Nigeria. *Environmental Monitoring and Assessment*, 193(12), 821. https://doi.org/10.1007/s10661-021-09477-1.

Fetter, C. W., Boving, T., & Kreamer, D. K. (2018). *Contaminant Hydrogeology* (3rd ed.). Waveland Press. ISBN: 978-1478637292.

Freeze, R.A., & Cherry, J. A. (1979). Groundwater. Prentice–Hall Inc., Englewood Cliffs 7632, 604. ISBN: 978-0133653120.

Garba, I., Okunlola, O. A., & Adekeye, J. I. D. (2021). *Geology and Geochemical Characterization of the Biotite Granites from the Jos-Bukuru Complex, Nigeria: Implications for Sn-Nb-Ta Mineralization*. Journal of African Earth Sciences, 179, 104201. https://doi.org/10.1016/j.jafrearsci.2021.104201.

Geological Survey of Nigeria (GSN). Geological map of Plateau State. (2006).

Gibbs, R.J. (1970). Mechanism controlling the world's water chemistry. *Science* 170, 1088–1090. https://doi.org/10.1126/science.170.3962.1088.

Graham, J. P., & Polizzotto, M. L. (2021). *Pit Latrines and Their Impacts on Groundwater Quality: A Systematic Review*. Environmental Health Perspectives, 129(6), 066001. https://doi.org/10.1289/EHP8185.

Horton, R. K. (1965). "An Index Number System for Rating Water Quality" *Journal of the Water Pollution Control Federation*, Vol. 37, No. 3, 300-306.

Jiang, S., Li, J., Wang, B., Wang, Y., He, M., & Wang, X. (2023). A review of advanced materials for calcium and magnesium ion removal in water softening: Performance and mechanisms. *Journal of Water Process Engineering, 53*, 103709. https://doi.org/10.1016/j.jwpe.2023.103709.

Karunanidhi, D., Aravinthasamy, P., Subramani, T., Srinivasamoorthy, K., & Prakash, M. (2021). Risk of fluoride-rich groundwater on human health: geochemical modeling and bio-statistical assessment. *Environmental Monitoring and Assessment, 193*(2), 1-18. https://doi.org/10.1007/s10661-021-08874-w.

Karunanidhi, D., Aravinthasamy, P., Subramani, T., & Anand, B. (2022). Revealing drinking water quality issues and possible health risks based on water quality index (WQI) method in the Shanmuganadhi River basin, South India. *Environmental Geochemistry and Health, 44*(2), 495-525. https://doi.org/10.1007/s10653-021-01048-0.

Li, J., Zhang, Y., Ma, L., Huang, S., & Li, Y. (2022). The relative impacts of anthropogenic activities and population density on river water quality in a coastal city of China. *Journal of Cleaner Production,367*, 133027.

McQueen, R. H., & Terhaag, D. (2021). Sustainable laundering conditions: The influence of washing machine program and detergent on fiber release and fabric care. *Textiles*, 1(2), 242-256. https://doi.org/10.3390/textiles1020012.

National Bureau of Statistics (NBS). (2020). *Demographic Statistics Bulletin 2020*. National Bureau of Statistics, Nigeria. https://nigerianstat.gov.ng.

Piper, A. M (1944). A graphic procedure in the geochemical interpretation of water analysis. *Trans American Geophysics Union* 25(6), 914-923.

Plateau State Nigerian Civil Conflicts Committee (PNCC). (2022). *Plateau State Peace and Security Project: Environmental and Conflict Analysis*.

Selvakumar, S., Ramkumar, K., Chandrasekar, N., Samuel, V. N., & Rajakumar, S. (2017). Hydrogeochemical characteristics and groundwater contamination in the rapid urban development areas of Coimbatore, India. *Water Resources and Industry, 17*, 26–33. https://doi.org/10.1016/j.wri.2017.02.002.

Sener, S., Sener, E., & Davraz, A. (2022). Assessment of water quality using water quality index (WQI) method and GIS in Aksu River (SW Turkey). *Environmental Science and Pollution Research*, 29, 1233–1245. https://doi.org/10.1007/s11356-021-15789-z.

Tiwari, A. K., Singh, P. K., & Mahato, M. K. (2021). GIS-based evaluation of water quality index of groundwater resources in West Bokaro Coalfield, India. *Journal of Geology, Geography and Geoecology*, 30(1), 1-10. https://doi.org/10.15421/112101.

Turner, D. C., & Bowden, P. (2021). *The Geology of the Younger Granite Complexes of the Jos Plateau, Nigeria*, *Bulletin, 32,* 1–105.

Uddin, M. G., Nash, S., & Olbert, A. I. (2021). A review of water quality index models and their use for assessing surface water quality. *Environmental Science and Pollution Research*, *28*, 3200–3225. https://doi.org/10.1007/s11356-020-11296-w.

UN-Water. (2022). *The United Nations World Water Development Report 2022: Groundwater: Making the invisible visible*. UNESCO. https://doi.org/10.18356/9789210014871.

Ustaoglu, F., & Tepe, Y. (2023). Water quality and sediment contamination assessment of the Pazarsuyu Stream in Turkey using multivariate statistical methods and pollution indicators. *International Journal of Environmental Science and Technology*, 20, 1–18. https://doi.org/10.1007/s13762-023-04795-y.

World Bank. (2022). *The Hidden Wealth of Nations: The Economics of Groundwater in Times of Climate Change*. https://openknowledge.worldbank.org/handle/10986/37237.

Zhang, Y., Dai, Y., Wang, Y., Huang, X., Xiao, Y., & Pei, Q. (2021). Hydrochemistry, quality, and potential health risk appraisal of nitrate-enriched groundwater in the Nanchong area, southwestern China. *Science of The Total Environment, 784*, 147186. https://doi.org/10.1016/j.scitotenv.2021.147186.